NEOPLASIA
www.neoplasia.com
Volume 22 Number 12 October 2020 pp. 809-819

Injured tissues favor cancer cell implantation via fibrin deposits on scar zones

Iman Al dybiat [a]; Shahsoltan Mirshahi [b]; Meriem Belalou [a]; Djedjiga Abdelhamid [a]; Shahid Shah [a]; Matti Ullah [a]; Jeannette Soria [a]; Marc Pocard [a]; Massoud Mirshahi [a,*]

[a] CAP-Paris Tech, INSERM U1275, UniversitÅ de Paris, LariboisiÉre Hospital, 2 rue Ambroise ParÅ, 75010 Paris, France; [b] Diagnostica Stago, 125 Avenue Louis Roche, 92230 Gennevilliers, France

Abstract

Aim: Evaluation of fibrin role on cancer cells implantation in injured tissues and studying the molecular mechanism of cancer cell interaction with the peritoneal damage.

Material and methods: Mouse colon cancer (CT26) and human mesothelial cells (HMCs) were used. CT26 cells were implanted on injured peritoneal zones. Icodextrin was used as a lubricant. For *in vitro* studies, fibrin clots from human plasma were used. The cell-fibrin interaction was observed by optical, electronic, and confocal microscopies. Aprotinin was used as a plasmin inhibitor. Hemostasis impact quantified by (1) the fibrin degradation product D-Dimer and PAR expression in HMCs; (2) the expression of plasminogen activator (PA) and its inhibitor (PAI-1) in cancer cells by qPCR and in supernatants through ELISA after *in vitro* HMC incubation with 2U of thrombin for 24 h.

Results: (i) Cancer cell lines were adhered and implanted into the wound area *in vivo* in both the incision and peeling zones of the peritoneum and on the fibrin network *in vitro*. (ii) Icodextrin significantly inhibited cancer nodule formation in the scar and the incision or peritoneal damaged zones after surgery. (iii) In *in vitro* studies, cancer cell interaction with the fibrin clot generated a lysed area, causing an increase in plasmin-dependent fibrinolysis measured by D-dimer levels in the supernatants that was inhibited by aprotinin. (iv) Aprotinin inhibited cell-fibrin interaction and invasion. (v) Thrombin upregulates PAI-1 and downregulates PA expression in HMC.

Conclusion: Injured tissues favor cancer cell implantation through generated fibrin. Fibrin-cancer cells adhesion can be inhibited by icodextrin.

Neoplasia (2020) 22 809–819

Introduction

Recurrence and intra-abdominal tumor cell spread are major concerns for abdominal peritoneal metastasis in ovarian, colon or gastric cancer. The most frequently affected area is the former location of the primary tumor resection site and the peritoneum at traumatized site [13]. That any tissue traction or peritoneal damage can increase the risk of recurrence has been established in previous studies [23,33] . Tissue and wound healing are related to specific growth factors that are associated with cancer cell implantation and growth [45]. The scars created after injury are always associated with immune inflammatory stimulation, adhesion and activation of platelets, and fibrin formation [28,14]. Thrombin, coagulation factor II, which is generated by procoagulant activity and expressed by

Abbreviations: CT26, mouse colon cancer cell line, HMCs, human mesothelial cells, PA, plasminogen activator, PAI-1, plasminogen activator inhibitor, PAR, protease-activated receptors, qPCR, quantitative polymerase chain reaction, ELISA, enzyme-linked immunosorbent assay, DMEM, dulbecco's Modified Eagle Medium, ATCC, American Type Culture Collection, PBS, phosphate-buffered saline, PCI, peritoneal *Cancer* Index, SEM, scanning electron microscope, PFA, paraformaldehyde, NETs, neutrophil extracellular traps, uPA, urokinase plasminogen activator, tPA, tissue plasminogen activator, CTRL, control

* Corresponding author: CAP-Paris Tech, INSERM U1275, UniversitÅ de Paris, LariboisiÉre Hospital, 2 rue Ambroise ParÅ, 75010 Paris, France.
e-mail addresses: iman.aldybiat@inserm.fr (I. Al dybiat), shah.mirshahi@inserm.fr (S. Mirshahi), jeannette.soria-ext@aphp.fr (J. Soria), marc.pocard@inserm.fr (M. Pocard), massoud.mirshahi@inserm.fr (M. Mirshahi).

https://doi.org/10.1016/j.neo.2020.09.006

inflammatory cells, plays a crucial role in the transformation of fibrinogen to fibrin and the modification of clot microenvironment homeostasis [3]. The clot formed on injured tissue following tumor resection initially serves to inhibit bleeding and contains several adhesion proteins such as fibronectin [42,41]. In previous work [29], we reported the expression of procoagulant and proteolytic enzymes within the tumor microenvironment modifies peritoneal surfaces during carcinomatosis growth; in *in vitro* studies, we showed that fibrin clots could serve as a niche for cancer implantation and expansion. Here, using an *in vivo* study and the murine colon cancer cell line CT26 in an *allograft* model, we analyzed the impact of tissue injury following surgical intervention (incision) or peritoneal surface damage on cancer cell adhesion and dissemination.

Materials and methods

Cancer cell lines: The murine colon cancer cell line CT26 and normal adult human mesothelial cells HMCs were purchased from the American Type Culture Collection ATCC (Manassas, VA, USA) and Zen Bio, Inc. (Research Triangle Park, North Carolina, USA), respectively. CT26 cells and HMCs were maintained in DMEM medium (Gibco, Saint Aubin, France) and mesothelial cell growth medium (ZenBio, Inc.), respectively. Cells were cultured in type 75 flasks in respective culture medium containing 1% penicillin–streptomycin, 1% L-Glutamine (Gibco, Saint Aubin, France) and 10% fetal calf serum at 37 °C, 5% CO_2 and 80% humidity. Mesothelial cells were cultured in type 75 flasks in the corresponding culture medium containing 1% penicillin–streptomycin, 1% L-glutamine and 20% fetal calf serum (Gibco, Saint Aubin, France). The culture medium was renewed every 48–72 h. Once the confluence reached 75–80%, the cell supernatant was discarded, and the adherent cells were washed with 1% PBS buffer and then detached from the flask using 2 ml of 1% trypsin (Sigma, St. Quentin Fallavier, France) for 2 min incubation at 37 °C. The trypsin enzyme activity was stopped by adding the corresponding culture medium, and then the cell suspension was centrifuged for 5 min at 1500 rpm in a 15-ml flacon (Sarstedt, Marney, France) Cells were counted using C-Chip slides (Labtech, East Sussex, UK).

Animals: Thirty female Balb/C mice (four weeks old) were purchased from Charles River Laboratories (Arbresle, France), with body weights ranging from 20 to 25 g. All the animals were maintained at the animal facility for 2 weeks of adaptive feeding before the start of the experiment. The animals were randomly divided into groups. The mice were caged in groups of 5 per cage in an air-filtered laminar flow cabinet and fed with irradiated food and autoclaved reverse-osmosis-treated water. All procedures were performed under sterile conditions in a laminar flow hood. The experimental protocol was approved by the Ethics Review Committee for Animal Experimentation of UPMC, France (APAFiS Number 3944). All the experimental protocols were performed in accordance with the European Convention for the protection of vertebrate animals used for experimental and other scientific purposes (Council of Europe, 1986, ETS No. 123).

Tumor and injury induction: Thirty Balb/C mice in 6 cages (5 mice per cage) were used for the first experiment. All the mice were operated (2 cm incision) on the abdominal side after skin disinfection with Betadine (Vetoquinol SA, France) and then were inoculated with 10^5 CT-26 cells in 200 µl of DMEM to create a limited peritoneal implant. Next, the mice were divided into three group. The first group (10 mice) had a tumor graft only (10^5 CT26 murine cells were injected intraperitoneally into the mice after anesthetization with 2% isoflurane in oxygen with mechanical ventilation for 15 min). The second group (10 mice) had a tumor graft and peeling on the peritoneal wall; injury was induced by scraping using sterilized Q-tips (Eseb, Brescia, Italy) on the right and left internal sides of the peritoneal wall. The third group (10 mice) had a tumor graft and injury induction and anti-adhesion (icodextrin 4% (Adept®; Baxter Healthcare S.A.) injection with injury induction; 100 µl of icodextrin 4% was injected intraperitoneally per mouse (Table 1). The mice were monitored for 2–3 weeks to check the development of tumor nodules.

Tumor evaluation

1- Because CT26 cells express luciferase CT26-Luc, the tumors were followed using an optical imaging bioluminescence camera one and two weeks after the injection day (camera: IVIS Lumina and IVIS Lumina II (Caliper). Next, 200 µl of Firefly D-Luciferin (15 mg/mL) diluted in PBS 1% (Life Sciences, Carbonne, France) was injected intraperitoneally into the mice. Ten minutes after injection, the anesthetized mice were placed in a luminescence measurement chamber and bioluminescence images were taken after 5 min. The results were evaluated using the sum of photons/cm^2/second/steradian (ph/cm^2/s/sr) and Piper Luminous software. The regions of interested (ROIs) were plotted (ROI, abscissa x = 199, y = 119).
2- Peritoneal cancer index (PCI score): The PCI was adapted to fit the animal model: Immediately after sacrificing the mice, the (PCI) was used to assess the extent of peritoneal cancer throughout the peritoneal cavity. For this purpose, the peritoneal cavity is divided into thirteen well-defined regions (8 in the peritoneum and 4 in the bowel). In each of the thirteen regions, the size of the tumor nodule was measured. If no tumor was visualized, a score of zero is given to that region: ``1'' if the tumor tissue was <2 mm, ``2'' if the tumor was between 2.1 and 5 mm and ``3'' if the tumor was >5 mm [32,12].

Sample collection

1- *Ex vivo* animal samples: After mouse sacrifice and PCI measurement, 2–4 cm of the peritoneal wall in both sides, including the injured area and stitched area of the peritoneum, was collected. The samples were stored in 4% PFA (Sigma-Aldrich, St. Quentin Fallavier, France) at 4 °C for scanning electron microscopy and histochemistry analysis.
2- Human *In vivo* samples: Peritoneum fragments from colorectal cancer patients were obtained from the General and Digestive Tract Surgery Department at LariboisiÉre Hospital in Paris (France). Informed consent was obtained from each patient before surgery. The membranes were elongated on a polystyrene piece, fixed with 4% PFA and store at 4 °C.

Scanning electron microscopy

Two preparation methods were used for peritoneal samples:

1- The peritoneal membranes were fixed using 4% formaldehyde for 24 h. and washed with 1× PBS buffer three times for 5 min each. Thereafter, 2.5% glutaraldehyde was added to the membrane for 20 min and washed with 1× PBS buffer three times for 5 min each. After a final wash in distilled water, the samples were dehydrated using increasing concentrations of ethanol (50%, 70%, 90%, and 100%). The samples were sputter-coated with gold or platinum after drying using the EMSCD500 apparatus from Leica. The samples were observed using an SEM FEG ZEISS ultra 55 scanning electron microscope equipped with a LaB6 filament operating at 15 kV, and images were captured using ``Orion'' software (NCH Software).

Table 1. Experiment plan for tumor production and injury induction.

Group (10 mice)	Incision	Peeling	Icodextrin 4%	CT26 injection
A	+	−	−	+
B	+	+	−	+
C	+	+	+	+

2- Peritoneal membranes were prepared via by critical point drying (CPD) using the Leica EMCPD300 apparatus. The concept is to change the state of the tissue from liquid to gas, preserving the surface structure of a specimen from damage due to surface tension. Fixed peritoneal samples (1 cm) were dehydrated in several successive ethanol baths (at 50%, 70%, 90%, 100%) for 5 min for each concentration with agitation after being incubated with 2.5% glutaraldehyde for 20 min and washed with 1× PBS buffer three times for 5 min each. The samples were prepared with 20 cycles and 100% methanol. The samples were sputter-coated with a platinum layer after drying using the Leica EMSCD500 apparatus.

Histochemistry analysis: The fixed samples were embedded in paraffin, and then the samples were sliced into 4 microns and fixed on slides (Surgipath Apex; Leica Microsystems, Germany) and stained with hematoxylin-eosin-saffron according to classical methods in the anatomopathological laboratory (Lariboisiere Hospital) and monoclonal anti-fibrin (F1E1 [31] and anti-plasminogen receptor [16]). The slides were evaluated, and pictures were taken using a Leitz (Diaplan) microscope with a Nikon Coolpix 995 camera (Japan).

Clot study

1- *In vitro* study: The objective of this manipulation was to study the behavior of CT26 cells on fibrin. Fibrin was obtained by adding thrombin (diluted in 0.025 M $CaCl_2$) at 5 units/mL to normal plasma and mixing immediately to avoid coagulation before being deposited in the wells of the sterilized culture cell plate. For clots, 80 µL of the mixture was added to each well of a 6-well microplate. Once the clots were formed, the CT26 cell suspension (10,000 cells) was deposited in each well. Next, culture medium was collected every 24 h. Some wells were treated with anti-plasmin by adding aprotinin (1/100) to the culture medium. In parallel and to verify whether fibrin lysis is plasmin dependent, fibrin clots were incubated with anti-trypsin in a dose-dependent manner (1/10,1/100, 1/1000).

Di-dimer measurement: To analyze fibrin degradation by CT26 cells, the D-dimer level was evaluated in the liquid present above the fibrin deposit using STAR-Liastest D-DI PLUS (Stago, Gennevilliers, France).

1.2

Micro cinematography: To analyze the kinetics of CT26 cells in the presence of fibrin, time-lapse microcinematography was performed as follows: the plate containing the clots with CT26 cells was placed on the top of the environmental chamber. Microcinematography was performed by acquiring images every 2 min for 24 h to determine the migration of CT26 cells on fibrin deposits in a temperature-controlled room of 37 °C in a humidified atmosphere (>80%) containing 5% CO_2 using an EVOS® FL Auto Imaging System (Life Technologies™, Waltham, USA). The migration of cancer cells was expressed in micrometers/min.

2- *In vivo* study:

2.1

In mice inoculated with CT26 cells, the presence of fibrin in the peritoneum was identified by adding F13P peptide 1 mg/ml that derived from alpha-2 antiplasmin protein and that binds to fibrin: the F13P peptide [NH2]GNQEQVSPLTLLK-Cys (Alexa 488) [COOH] sequence for *in vitro* study and [Alexa700]GNQEQVS PLTLL[COOH]sequence for *in vivo* study (ThermoFisher, Villebon sur Yvette, France). Before using the peptide in an animal model, the labeled F13 peptide was checked *in vitro* first with fibrin clots. The protocol used was as follows. For *in vitro* detection, the F13 peptide at 1 mg/mL was diluted in DMSO (0.5 mg/ml), and then 1 µl of the diluted labeled F13 was added to 2 ml of culture medium per well. After 2 h of incubation, the wells were washed three times for 5 min and then the samples examined by immunofluorescence microscopy (EVOS Life Technologies™, Waltham, USA) and by confocal microscopy (ZEISS; LSM 800). The samples were imaged by confocal microscopy (after adding F13 peptide Alexa 488 to fibrin droplets prepared by Labtech (Clinicscience, Nanterre, France) using Zeiss Immersol™ Immersion oil 518F (Carl Zeiss, Oberkochen, Germany) at × 63 magnification.

For *in vivo* detection, 5 female Balb/C mice aged 7 weeks were injected intraperitoneally with 50×10^3 CT26 cells. Three of these mice had injury induction on the internal side of the peritoneal wall in addition to CT26 injection. The two others were injected with CT26 only and not in the incision area. Five days later, 100 µl of diluted F13P was injected intraperitoneally per mouse for fibrin detection by the luminescence signal due to the interaction of labeled peptide binding to fibrin (Table 2).

Quantitative qPCR

For qPCR studies, human mesothelial cells were incubated in 2 units of thrombin (Stago, Gennevilliers, France) that been added to serum-free conditioned HMC culture medium. To discard the thrombin from culture medium, twelve hrs later, the culture medium has been changed and cells were incubated again twenty-four hours with the serum-free conditioned HMC culture medium. total RNA was extracted using the RNA extraction kit for cells (Z6011; Promega, Madison, USA) according to the manufacturer's instructions. Cells incubated without thrombin addition to the culture medium were considered the control. RNA samples were first transcribed to cDNA (Thermo Scientific cDNA synthesis kit #K1671) and then the requested primers were standardized as follows: a mixture of 5 µL of SYBR MasterGreen (FastStart Essential DNA Green Master SYBR, Roche, Mannheim, Germany) containing an identical quantity of forward and reverse primers and 2.5 µL of a decreasing concentration of cDNA from 1 to 0.001 ng/mL. Primers with an R-sq value of 1.00 and an efficiency between 1.90 and 2.10 were selected for qPCR. Using the QuantiTect reverse transcription kit (Thermo Fisher Scientific Inc, Waltham, USA) and LightCycler 480 multiwell plate 96 (Roche, Mannheim, Germany), 0.5 µL each of forward and reverse primers was added to 2.5 µl of cDNA at 1 ng/µL. The plate was covered using a special film (AB1170; Thermo Fisher Scientific, USA) to protect the wells, and then it was centrifuged for 1 minute at 1000 g before lancing the thermocycler with the following conditions: 94 °C for 2 min, followed by 40 cycles (denaturation for 15 s at 95 °C, annealing for 20 s at 60 °C) and extension for 20 s at 72 °C). The primer sequences and PCR product size for the target and reference genes are listed in Table 3 with Þ-actin as an internal reference.

Table 2. Experiment plan for *in vivo* fibrin deposit detection.

Group	Mouse number	Incision	scratching	CT26	F13P injection
A	3	+	+	+	+
B	2	−	−	+	−

Table 3. Primers sequences and PCR product size.

Gene name	5′ Forward 3′	3′ Reverse 5′	Product size
Beta-Actin	AGAGCTACGAGCTGCCTGAC	AGCACTGTGTTGGCGTACAG	184
u-PA	TCACCACCAAAATGCTGTGT	AGGCCATTCTCTTCCTTGT	223
PAI-1	CTCTCTCTGCCCTCACCAAC	GTGGAGAGGCTCTTGGTCTG	212
PAR 1	GTGATTGGCAGTTTGGGTCT	GCCAGACAAGTGAAGGAAGC	178
PAR 2	CTGCATCTGTCCTCACTGGA	CAG GAGGAGGTCAGCCAAG	180

The PCR products of HMC cell samples after qPCR were electrophoresed using a 2% agarose gel electrophoresis system (Thermo Fisher Scientific Inc., Waltham, USA).

Enzyme-linked immunosorbent assay (ELISA)

Human mesothelial cells were incubated in 2 units of thrombin (Stago, - Gennevilliers, France) that had been added to serum-free conditioned HMC culture medium. To discard the thrombin from culture medium, twelve hrs later, the culture medium has been changed and cells were incubated again twenty-four hours with the serum-free conditioned HMC culture medium. The culture medium was collected for protein measurement. Incubated cells without thrombin addition to the culture medium were considered the control. Urokinase plasminogen activator (uPA) and plasminogen activator inhibitor (PAI-1) evaluations were performed using ELISA kits (Sigma-Aldrich, Saint-Quentin Fallavier, France), Tissue plasminogen activator (t-PA) evaluation was performed using Asserachrom® t-PA (Diagnostica Stago, Asnieres, France).

Statistical analysis

The data were analyzed using the nonparametric Mann–Whitney test with GraphPad Prism 6 Software. P-values less than 0.05 were considered significant.

Results

CT26 cancer cells induce cancer nodule formation in the injured zones of the Balb/C mouse model

Twenty mice were divided into two groups (10 mice per group) with incision only in the first group and scratching in addition to the incision in the second group. Fig. 1A shows the mouse with the incision area in the middle of the abdomen and the scratching zones bilaterally performed on the internal side of the peritoneal surface (marked with star). Nodule formation after 7 and 14 days (D-7 and D-14 respectively) of CT26 intraperitoneal injection in both groups was followed via bioluminescence assay Figure B (D-7, D-14). High bioluminescence expression was observed in the group with both incision and peritoneal peeling ($P < 0.05$). The peritoneal cancer index (PCI) was used to assess the extent of peritoneal cancer at the end of the experiment (14 days). Fig. 1C1 describes tumor nodule dissemination inside the abdomen two weeks after injection. Mice with scratching showed a significant increase in PCI Fig. 1C 2. Tumor nodules formed at the incision site in both groups, as well as in the mesothelial cell peeling areas in the second group with bilateral peeling areas Fig. 1D-1, D-2. These results confirm cancer cell implantation and tumor mass formation on the damaged tissue of the peritoneum.

Icodextrin inhibits cancer cell adhesion to damaged zones of the peritoneal wall (in vivo mouse model)

After the incision of the peritoneum and induction of peritoneal scratching, 100 µl of icodextrin 4% was injected intraperitoneally at the same time of CT26 injection. Seven and fourteen days after the injection, bioluminescence evaluation was performed to evaluate tumor progression and nodule formation. Fig. 2A 1 shows the areas of cancer cell adhesion after 7 and 14 days of injection. This expression was increased when the peritoneal surface was experimentally scratched, and the mesothelial layer was ablated. Under the same experimental condition, when icodextrin was used, the bioluminescence-expressed signal of cancer cells was significantly reduced compared with the incision-only group Fig. 2A 2. The macroscopic view of the peritoneum and incision zones confirmed the role of icodextrin in decreasing tumor expansion while expanding to both sides of the peritoneum in the incision group without icodextrin treatment Fig. 2B 1. The PCI score showed a significant difference among the three groups after icodextrin treatment Fig. 2B 2.

Fibrin deposits are generated on the peritoneum after mesothelium peeling

To evaluate fibrin deposits on the peritoneum by mesothelial cell peeling, we used a fibrin tracer (labeled F13 peptide (an anti-plasmin) with a green tracer (AF-488 fluorochrome) used for *in vitro* study and a red tracer (with AF 700 Alexa) for *in vivo* exploration.

A- Using *in vitro* assays, the specific interaction of the fibrin tracer F13 with plasma clots are presented in Fig. 3. The fluorescence of the fibrin network is presented in Fig. 3A 1 and the confocal view in Fig. 3A 2. Using *in vivo* assays in mice, the red fibrin tracer identified by fluorescence imaging was observed in animals injected with CT26 to induce peritoneal metastasis. Fifteen minutes after the intraperitoneal injection of fibrin tracers, the kinetics of the peptide signal in mice with peritoneal metastasis was measured over time (after 20, 60, 80 and 120 min; Fig. 3B 1. Fig. 3B 2 shows injected mice on the left and control mice without any tracer on the right 20, 60, 80 and 120 min following tracer injection. Both mouse groups had peeling on the peritoneal side. After 55 min, the interaction of the fibrin tracer with fibrin deposits on the peritoneal surface was established and the areas with fibrin deposits were identified. The peritoneum areas with detected fibrin and small nodules were removed and analyzed by fluorescence Fig. 3C. The red signal of the fibrin tracer on the peritoneal surface indicates fibrin deposits Fig. 3C 1. Fig. 3C 2 is a contrasted photo that shows the nodule position in the middle, and Fig. 3C 3 presents the control without the fibrin tracer. These results indi-

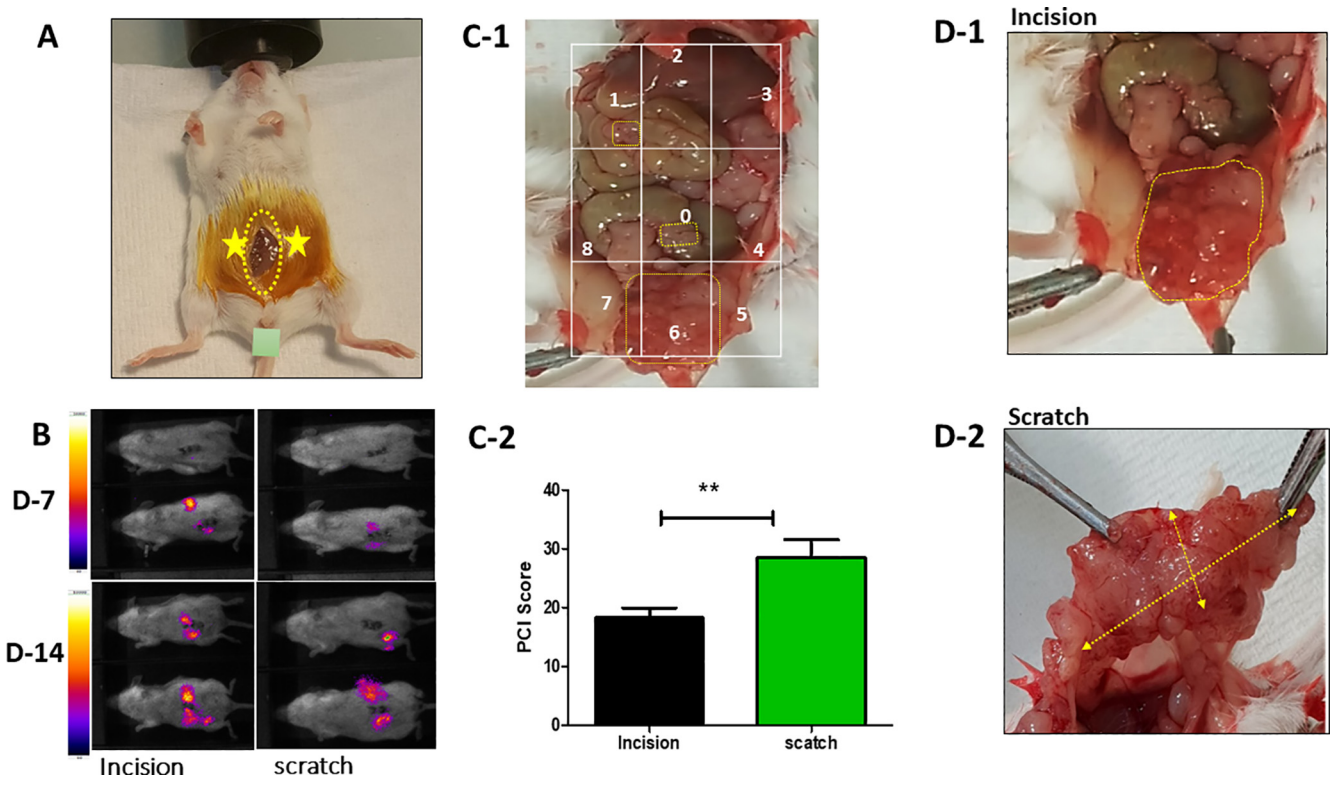

Fig. 1. Nodule formation and peritoneal metastasis in the *in vivo* model. A) Surgical zones in a Balb/c mouse: the incision zone is indicated by the yellow dotted line in the middle, and the two injured zones of the peritoneum are by yellow stars on the right and left sides of the peritoneum. B) Tumor monitoring by bioluminescence assay 7 and 14 days (D-7 and D-14) post-injection for both groups (with incision and with incision + peritoneal peeling). C-1 Peritoneal cancer index (PCI) of a Balb/c mouse with peritoneal metastasis showing different regions from 0 to 8 (9 to 12 are noticed once the intestine is disassociated). C-2 The PCI shows a significant difference between the groups with an increased PCI when the mice had a scratch zone beside the incision ($P < 0.0142$). D-1 A mouse with an incision showing a tumoral mass in the stitched zone (incision). D-2 Tumoral zone prolongation through the scratch zones (from left to right) and crossing the incision zone.

cate that cancer cells are niched in fibrin deposits. This finding was further confirmed using an anti-fibrin monoclonal antibody on the peritoneal surface through immunohistochemistry. The macroscopic view of the nodule on the peritoneum is presented in Fig. 3D 1, and the nodule histology is shown in Fig. 3D 2. The presence of plasminogen receptor and fibrin was determined using specific antibodies (anti-plasminogen receptor and anti-fibrin) compared with the control with no tracer Fig. 3D 4-6 vs Fig. 3D 3. The induction of digestive carcinomatosis in the animal model is associated with the generation of fibrin deposits colocalized with cancer nodules on the peritoneal surface.

Fibrin deposits on the cicatrice zones or damaged area on the peritoneum favor cancer implantation

In the scarred area induced by incision during surgery or cell peeling, the fibrin network is a major element identified by electron microscopy. Fig. 4A shows a fiber network deposited on the peritoneal wall. Furthermore, Fig. 4B illustrates cancer cells adhering to fibrin deposits on the cicatrice zone. In Fig. 4C, the tumor nodule can be seen on the peritoneal surface with fibrin deposition surrounding as well as inside the nodules. This can be seen more clearly at high magnification Fig. 4C 1 and 1a fibrin nets are observed in the attachment zone to the peritoneum surface through the nodule. Fig. 4C 2 shows fibrin inside the nodule.

These results suggest that the scar areas are associated with fibrin deposits where cancer cells adhere and proliferate. In parallel, the fibrin deposits on the peritoneal surface are not degraded. Fibrin generation via thrombin is associated with fibrinolysis. Here, we observed that, even after two weeks, fibrin deposits are not degraded.

Role of thrombin in the fibrin network integrity of peritoneal mesothelial cells

The peritoneum surface is a non-adhesive membrane. Under pathologic conditions, such as induced damage of the mesothelial layer, fibrin is generated via the thrombin-PAR activation pathway. This fibrin persists on the peritoneal membrane as we observed in carcinomatosis. To better understand this mechanism, we used human mesothelial cells and studied the role of thrombin as a physiological coagulation inducer. Mesothelial cells naturally expressed mRNA for PAR-1 and PAR-2, and both proteins served as thrombin receptors on the mesothelial cells Fig. 5A. We also examined the mRNA expression of the plasminogen activator uPA and its inhibitor PAI-1 in the mesothelial cells Fig. 5B. *In vitro* studies revealed that thrombin (2 and 5 U) thrombin downregulates uPA Fig. 5C and upregulates PAI-1 Fig. 5D. These results favor losing fibrinolytic activity via mesothelial cells.

Cancer cell interaction with fibrin via plasmin generation

Fibrin droplets were identified as white spots. After clotting, the clots were incubated with culture medium only as the control Fig. 6A or with CT26 cells, followed by evaluation for 5 days Fig. 6B 2-4. In the wells with CT26 cancer cells, fibrin was degraded over five days; however, the

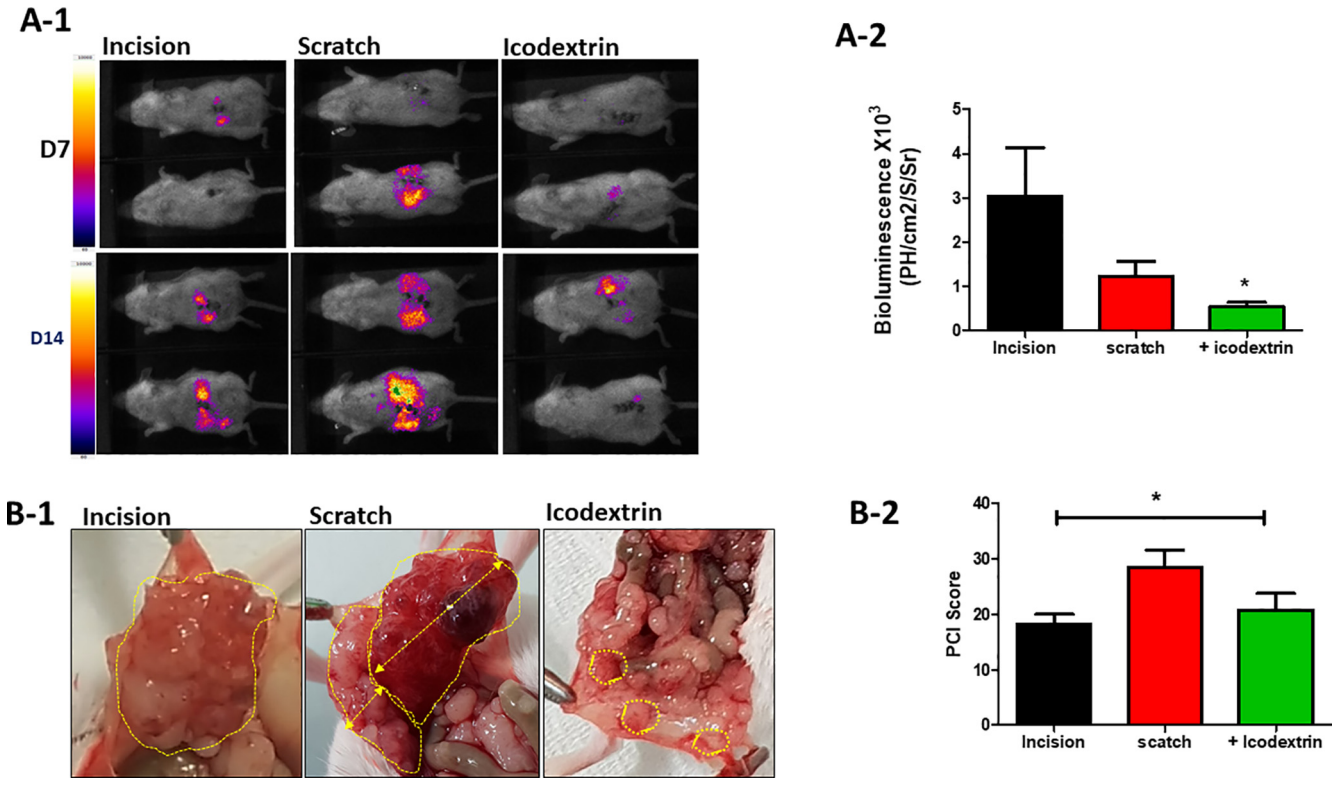

Fig. 2. Evaluation of Peritoneal metastasis after Icodextrin 4% injection. A-1 Bioluminescence signal of tumor formation 7 and 14 days after CT26 injection of the three groups (mice with an incision area on the right side, in the middle with peeling in addition to the incision and with Icodextrin treatment on the left side). A-2 Significant difference between the first mouse group with incision and the third mouse group with icodextrin treatment ($P < 0.0171$). No significance was observed between the peeling mouse group and the other groups. B-1 Macroscopic observations show the tumor distribution in the mice with icodextrin treatment compared with the group without treatment (incision and scratch). B-2 PCI shows a significant difference among the three groups with an increased tumor mass when the mice had a scratch beside the incision that decreased after icodextrin treatment.

addition of anti-plasmin `aprotinin' inhibited this fibrin lysis Fig. 6B 3 compared with the sample without aprotinin Fig. 6B 4 and showed similar clot formation to the control without cells Fig. 6B 2. Thus, the fibrinolytic process of cancer cells is plasmin dependent because fibrin lysis could not be blocked when the fibrin clots were incubated with anti-trypsin in a dose-dependent manner (1/10, 1/100, 1/1000) Fig. 6C1-3. Microscopic analysis of fibrin clots in the presence of anti-plasmin over time is presented in Fig. 6D. After 72 h, the cancer cells significantly degraded the fibrin clot compared with the control; anti-plasmin inhibited this reaction. Fibrin degradation in the study was confirmed by the quantification of fibrin degradation products by D-dimer analysis. After incubating the cancer cells with fibrin clots for one week, the D-Dimer levels were increased significantly ($P < 0.0193$) and confirmed the degradation of fibrin through plasmin Fig. 6E 1. In the presence of anti-plasmin, fibrin degradation products were not identified in the cell culture supernatant Fig. 6E 2 and was significantly lower than the levels found with CT26 cells ($P < 0.04$). The interaction between cancer cells and fibrin was further studied by scanning electron microscopy using the same samples Fig. 6F. Compared with the control without fibrin, when cancer cells were incubated with the fibrin clot, the clot border in the fibrin network was degraded Fig. 6F 1 and Fig. 6F 2. Fig. 6F 3 shows a cancer cell adhering to the fibrin clot. When aprotinin was added to the culture medium, the cells could not penetrate the fibrin clot; thus, they formed nodules on the fibrin surface Fig. 6F 4. The kinetics of the interaction between cancer cells and the fibrin network was investigated by microcinematography and confirmed the preceding observation (results not shown).

Discussion

Cancer cell metastasis in peritoneal cavity is known for more than one century [40]. This is the contrary of the mechanism of cancer cell adhesion and implantation into the peritoneum surface which needs to be more studied.

Here, we demonstrated that cancer cells adhere to and are implanted into the wound healing zones in an *in vivo* mouse model and in an *in vitro* study of the fibrin network. These observations are consistent with several clinical reports suggesting that intraoperative tumor manipulation can induce the dissemination of tumor cells in the peritoneal cavity.

The spread of tumor cells in the peritoneal cavity during surgery in cases of gastric carcinoma [10,36] , colorectal cancer [9,15,27] and pancreatic resection [7] as well as other surgical trauma [37] is associated with a poor prognosis.

In this work, we have studied the interaction of cancer cells with the fibrin network generated after the wound healing process. We found that fibrin degradation could be evaluated by an increase in fibrin degradation products (D-dimers). This observation can explain the high quantity of plasma D-dimer in cancer patients [19,30]. In our *in vitro* study, we revealed the role played by plasmin in the detachment of cancer cells from fibrin networks because aprotinin prevents the invasion of cancer cells by inhibiting fibrin network lysis. Previously, in human carcinomatosis, we observed fibrin deposition between the mesothelial cells of the peritoneal surface and implantation of cancerous nodules on fibrin [29]. Moreover, we have shown that these mesothelial cells can absorb human leukocyte

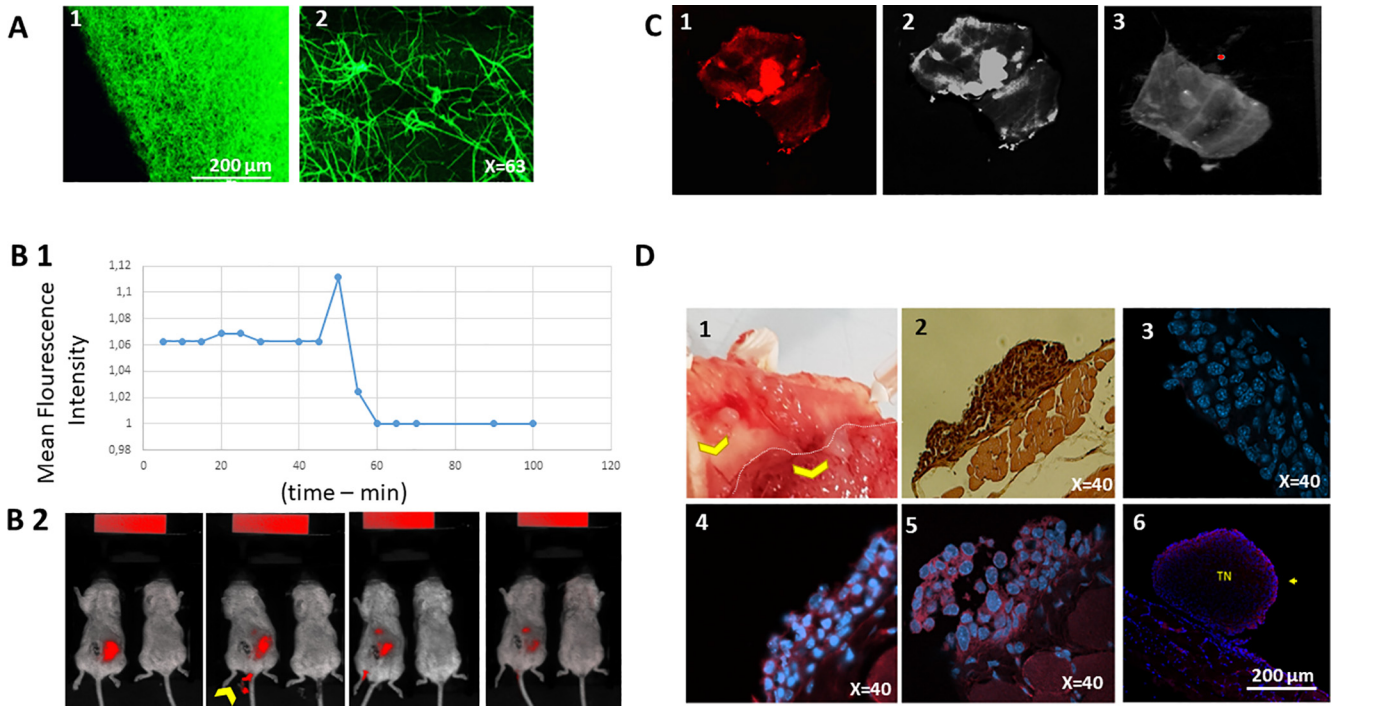

Fig. 3. Detection of fibrin in in vitro and *in vivo* mouse models. A-1 *In vitro* validation of the fibrin tracer F13 peptide 488 (anti-plasminogen) with a green signal when incubated with the fibrin clot. A-2 Confocal microscopy at higher magnification. B-1 Kinetics of the F13 peptide signal in mice with peritoneal metastasis 15 min after intraperitoneal injection. B-2 Localization of the injected peptide in the abdominal wall/cavity (red color) of the mouse left side, while the mouse right side is considered control where the peptide was not injected. The yellow arrow indicates peptide excretion (urine and feces). C-1 Fluorescence of the metastatic peritoneal area after peritoneum removal from the mouse and detection of peptide (red color). C-2 Tumor model area: the contrast phase shows the tumor as a white spot. C-3 The control shows the peritoneum without peptide injection; no red color was detected. D-1 The macroscopic photo shows the nodule on the internal face of the peritoneum. 2- The histochemistry photo shows the nodule on the peritoneal surface with some mesothelial cells detected; others are denodulated. 3- Immunofluorescence of the control nodule with no peptide treatment. Blue color indicates DAPI staining of the nucleus only. 4- IF photo of the nodule after anti-plasminogen antibody incubation (in red). 5- IF photo of anti-plasminogen at higher magnification. 6- IF photo of the nodule after anti-fibrin treatment. (For interpretation of the references to colour in this figure legend, the reader is referred to the web version of this article.)

antigen sHLA-G, which may provide immunoprotection to attach cancer cells [38]. Here, in an animal model, we reproduced the same phenomenon. Fibrin deposits on the peritoneal surface, which may constitute a niche for cancer cells, have also been observed in mice after the induction of carcinomatosis by gastric or ovary cancer cell implantation. In the inflammatory state, fibrinogen as a plasma exudate, excreted by the microcapillaries located in the inflammatory zone, is transformed into fibrin by local thrombin. The persistence of fibrin deposition observed in human carcinomatosis as well as in animal models can be ensured either by continuous local fibrin formation or by inhibition of the fibrinolytic enzymes u-PA and t-PA, which are activated by plasminogen activator inhibitors (PAI-1 and 2).

To study theses hypotheses, the action of thrombin on mesothelial cells was studied. We first showed the expression of the thrombin receptors PAR-1 and -2 by mesothelial cells. Thrombin treatment activated PAR and caused the upregulation of PAI-1 and downregulation of uPA expression, explaining the decrease in the fibrinolytic activity of mesothelial cells *in situ*. In another *in vitro* study, clot resistance to fibrinolytic agents was due to the presence of neutrophil extracellular traps (NETs) that were in the clots during fibrin formation [39].

When carcinomatosis is induced by the injection of cancer cells into the peritoneal cavity, the inflammatory microenvironment changes the shape of the mesothelial cells and creates an intercellular space in which fibrin deposition is observed. In the fibrin network, cancer cells can nest and generate multicellular agglomerates, leading to cancerous nodule formation. Many studies investigated the role of inflammatory microenvironment on enhancing cancer cells proliferation as in the study of [1] where they showed in translucent zebrafish larval model of Ras (G12V)-driven neoplasia that neutrophils are rapidly diverted from a wound to pre-neoplastic cells and these interactions lead to increased proliferation of the pre-neoplastic cells. This leads us to discuss the role of neutrophil cells on cancer progression [25] where the neutrophil extracellular traps NET's seems to promote cancer metastasis [4,2,43].

All observations indicated that fibrin generated after an injury, surgery or desquamation of the peritoneal surface might be a substrate for cancer cell adhesion. Several proteins, including fibronectin, were incorporated into fibrin during fibrin formation [21,42]. Fibronectin is involved in various cellular interactions with the extracellular matrix, such as fibrin, and plays an important role in cell adhesion, migration, growth and differentiation [17,18,6]. A normal clot is rich in fibronectin [35], which may be a target for cancer cell adhesion [26].

Because of the fibrin-cancer cell interaction, we cannot use anticoagulant or fibrinolytic molecules. Thus, a polysaccharide named icodextrin was used to inhibit cell interaction and adhesion of cancer cells to fibrin networks. In an *in vivo* model, we found that icodextrin significantly inhibited the formation of cancer cell nodules in the scarred area, as well as in incision or damaged peritoneum areas after surgery. Icodextrin, as a glucose polymer, is not metabolized significantly in the peritoneum. Instead, it is slowly absorbed into the blood by the lymphatic vessels [44]and is used as a primary osmotic agent at a concentration of 4% in

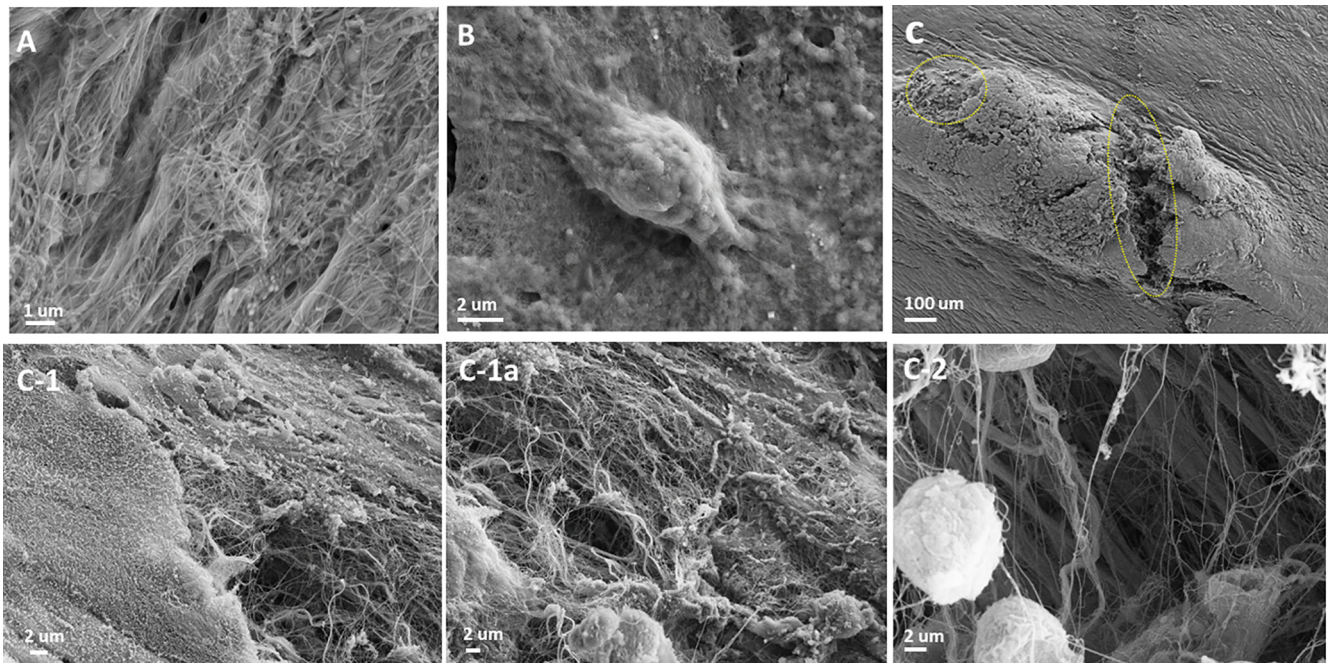

Fig. 4. Scanning electron microscopy study of fibrin deposition on the metastatic peritoneum. A- Fibrin deposition on the peritoneum. B- Cancer cell attachment with its pseudopods to the denodulated peritoneal surface. C- Tumor nodule with the detection of fibrin deposits on the border of the nodule and inside the nodule (yellow pointed area) C1. Border where fibrin was detected. C1a. At higher magnification. C2 Center of the nodule. (For interpretation of the references to colour in this figure legend, the reader is referred to the web version of this article.)

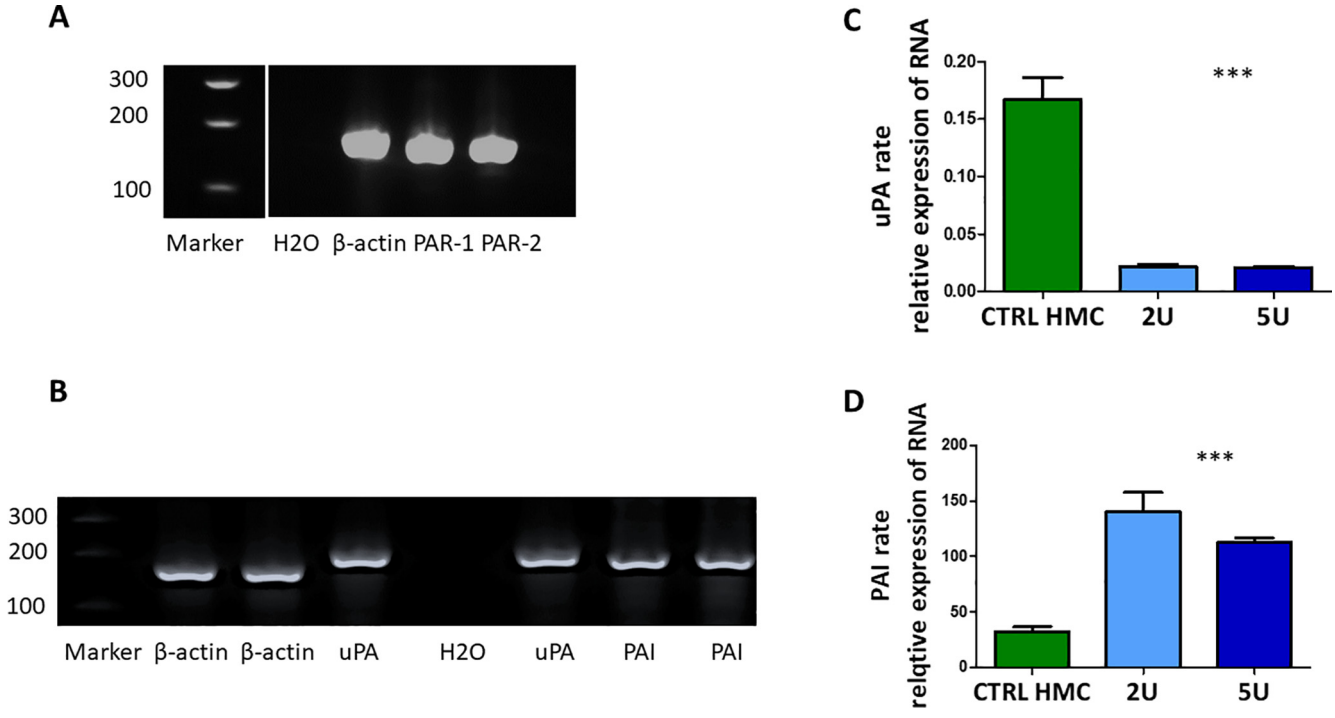

Fig. 5. Thrombin action on mesothelial cells. mRNA expression of PAR1 and 2 in mesothelial cells, mRNA expression of uPA and PAI-1 in mesothelial cells. β-Actin is a housekeeping gene used as a loading control. uPA downregulation after mesothelial cell stimulation with 2 and 5 U of thrombin PAI upregulation after mesothelial cell stimulation with 2 and 5 U of thrombin.

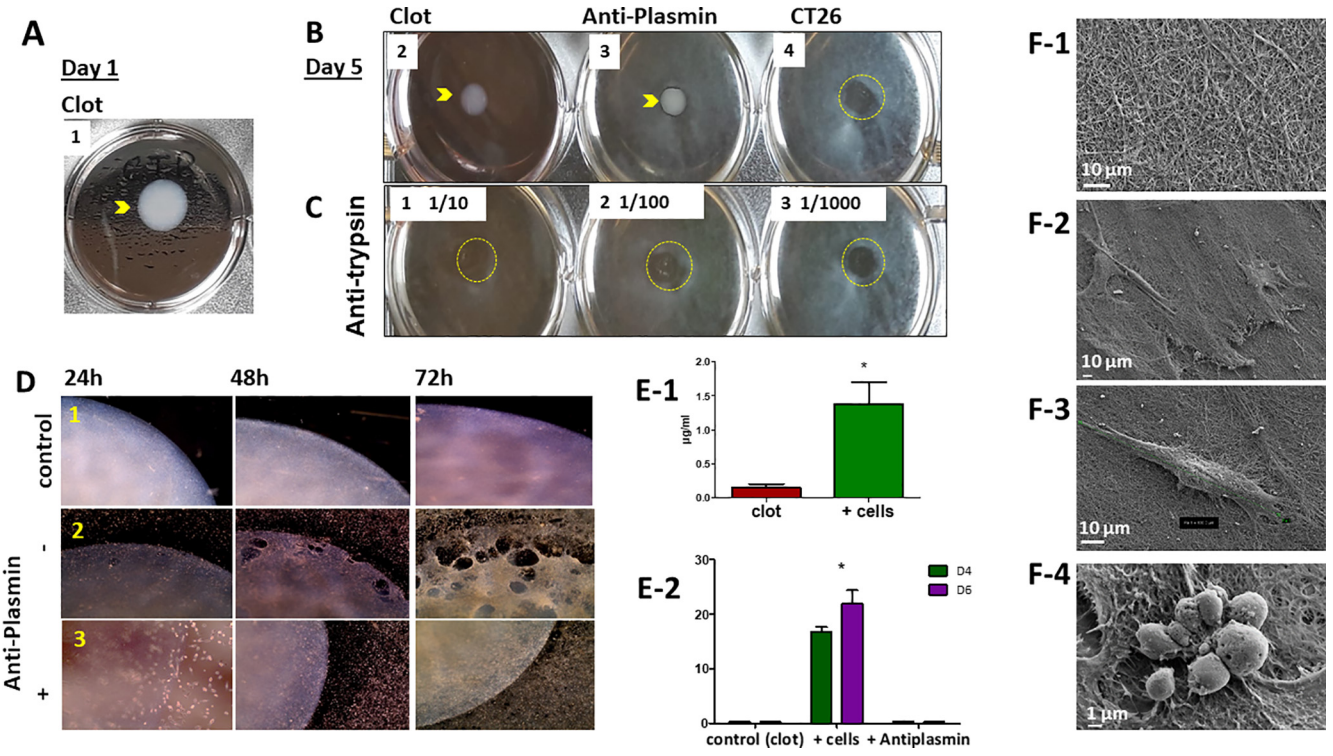

Fig. 6. *In vitro* Plasmin-fibrin degradation pathway. A) 1 Clot control incubated in culture medium after one-day incubation. B) Five days after incubation. B2) Clot control. B3) Clot incubated with aprotinin as an anti-plasmin enzyme. B4) Clot incubated with cancer cells. C1–3). Clot incubated with three different concentrations of anti-Trypsin enzyme. D) Microscopic images. D1) Clot incubated in culture medium after 24 h, 48 h and 72 h with a clear border. D2) fibrin degradation over time on the degraded border. D3) No degradation of the fibrin clot when incubated with anti-plasmin enzyme. Magnification × 4. E-1. Fibrin degradation via the measurement of product PDF (D-dimer) under two conditions (clot only and clot + cells) after four and six days of clot incubation with/without cells with a significant difference in the D-dimer level between the groups. $P < 0.0193$. $N = 3$. E-2. Fibrin degradation via the measurement of product PDF (D-Dimer) under three conditions (clot only, clot + cells, clot + cells + antiplasmin), with a significant difference among the three groups. $P < 0.04$. $N = 3$. F) Scanning electron microscopy view. F1) Fibrin clot, control. F2) Degraded border of fibrin clot when incubated with the cells. F3) Cancer cell with good adherence to the fibrin clot. F4) Cancer cells form a nodule on the clot surface when aprotinin, a plasmin inhibitor, was added to the culture medium; cells cannot penetrate the fibrin.

peritoneal dialysis solution [5,22,10–20]. Consequently, icodextrin may be a candidate for use during surgery to inhibit potential cancer cell expansion [11].

Independently of the surgical wound, peritoneal metastasis comes from different origins, such as vascular and lymphatic vessels or by a direct invasion. In all cases, an inflammatory reaction in the peritoneal environment could be produced and consequently, a niche for cancer cells on the peritoneal surface may be formed.

The peritoneum is relatively large in area, but the accessibility is limited for treatment, in the meantime it is easy for cancer cells dissemination. Therefore, different strategies have to be taken into consideration with the objective of gaining access to the entire surface of the peritoneum with less side effects or complications. Taking the choice of a strategy that inhibits implantation of cancer cells into the peritoneal cavity using a non-corrosive agent is very important.

Here we focused only on the application of icodecxtrin via intra peritoneal injection. Other methods such as Pressurized Intraperitoneal Aerosol Chemotherapy (PIPAC) method, that currently used in carcinomatosis chemotherapy, can be used for targeting the inhibition of cancer–fibrin adhesion [24,34,8].

In conclusion, fibrin deposition after peritoneal peeling in carcinomatosis, as well as in wounds after surgical incision, can be implicated as an important factor for the implantation and growth of tumor cells. These observations can be considered valid in all surgical incisions and also in inflammatory environments due to different pathologies.

On the peritoneal surface, locally generated thrombin induces peritoneal procoagulation activity responsible for fibrin formation and tumor regrowth. Hence, blocking the interaction between cancer cells and fibrin, through the use of surfactants such as icodextrin, may help to reduce cancer cell metastasis.

Authors contribution

Al dybiat Iman: Post doctorate and work realisator
Shahsoltan Mirshahi: Biological analysis
Meriem Belalou*: In vivo* experiment
Djedjiga Abdelhamid: *In vitro* experiment
Shahid Shah: Mesothelial cells impact
Matti Ullah: PCR and statistical analysis
Jeannette Soria: Biological analysis
Pocard Marc: Project collaborator
Mirshahi Massoud: Project director

Declaration of Competing Interest

The authors declare that they have no known competing financial interests or personal relationships that could have appeared to influence the work reported in this paper.

Acknowledgements

The authors gratefully acknowledge Mrs. Stephanie Delbrel and Mrs Franµoise Pillier UMR 8235 CNRS-UPMC - Interfaces and Electrochemical Systems laboratory for Scanning Electron Microscope SEM analysis.

References

1. Antonio N, BÖnnelykke-Behrndtz ML, Ward LC, Collin J, Christensen IJ, Steiniche T, Schmidt H, Feng Yi, Martin P. The wound inflammatory response exacerbates growth of pre-neoplastic cells and progression to cancer. *EMBO J* 2015;**34**(17):2219–36. https://doi.org/10.15252/embj.201490147.
2. Brostjan C, Oehler R. The role of neutrophil death in chronic inflammation and cancer. *Cell Death Discovery* 2020;**6**(1):1–8. https://doi.org/10.1038/s41420-020-0255-6.
3. Coughlin SR. Thrombin signalling and protease-activated receptors. *Nature* 2000;**407**(6801):258–64. https://doi.org/10.1038/35025229.
4. Erpenbeck L, SchÎn MP. Neutrophil extracellular traps: protagonists of cancer progression? *Oncogene* 2017;**36**(18):2483–90. https://doi.org/10.1038/onc.2016.406.
5. Frampton JE, Plosker GL. Icodextrin: a review of its use in peritoneal dialysis. *Drugs* 2003;**63**(19):2079–105. https://doi.org/10.2165/00003495-200363190-00011.
6. Fukuda T, Yoshida N, Kataoka Y, Manabe R-I, Mizuno-Horikawa Y, Sato M, Kuriyama K, Yasui N, Sekiguchi K. Mice lacking the EDB segment of fibronectin develop normally but exhibit reduced cell growth and fibronectin matrix assembly in vitro. *Cancer Res* 2002;**62**(19):5603–10.
7. Gall TMH, Jacob J, Frampton AE, Krell J, Kyriakides C, Castellano L, Stebbing J, Jiao LR. Reduced dissemination of circulating tumor cells with no-touch isolation surgical technique in patients with pancreatic cancer. *JAMA Surgery* 2014;**149**(5):482–5. https://doi.org/10.1001/jamasurg.2013.3643.
8. Girshally R, DemtrÎder C, Albayrak N, Zieren J, Tempfer C, Reymond MA. Pressurized intraperitoneal aerosol chemotherapy (PIPAC) as a neoadjuvant therapy before cytoreductive surgery and hyperthermic intraperitoneal chemotherapy. *World J Surg Oncol* 2016;**14**(1):253. https://doi.org/10.1186/s12957-016-1008-0.
9. Guller U, Zajac P, Schnider A, BÎsch B, Vorburger S, Zuber M, Spagnoli GC, et al. Disseminated single tumor cells as detected by real-time quantitative polymerase chain reaction represent a prognostic factor in patients undergoing surgery for colorectal cancer. *Ann Surg* 2002;**236**(6):768–76. https://doi.org/10.1097/00000658-200212000-00009.
10. Han T-S, Kong S-H, Lee H-J, Ahn H-S, Hur K, Yu J, Kim W-H, Yang H-K. Dissemination of free cancer cells from the gastric lumen and from perigastric lymphovascular pedicles during radical gastric cancer surgery. *Ann Surg Oncol* 2011;**18**(10):2818–25. https://doi.org/10.1245/s10434-011-1620-8.
11. Jouvin I, Najah H, Pimpie C, Canet Jourdan C, Kaci R, Mirshahi M, Eveno C, Pocard M. Reduction of carcinomatosis risk using icodextrin as a carrier solution of intraperitoneal oxaliplatin chemotherapy. *Eur J Surg Oncol (EJSO)* 2017;**43**(6):1088–94. https://doi.org/10.1016/j.ejso.2016.12.009.
12. Klaver YLB, Hendriks T, Lomme RMLM, Rutten HJT, Bleichrodt RP, de Hingh IHJT. Intraoperative hyperthermic intraperitoneal chemotherapy after cytoreductive surgery for peritoneal carcinomatosis in an experimental model. *Br J Surg* 2010;**97**(12):1874–80. https://doi.org/10.1002/bjs.7249.
13. Königsrainer I, Zieker D, Beckert S, von Weyhern C, Löb S, Falch C, Brücher BL, Königsrainer A, Glatzle J. Local peritonectomy highly attracts free floating intraperitoneal colorectal tumour cells in a rat model. *Cell Physiol Biochem* 2009;**23**(4-6):371–8. https://doi.org/10.1159/000218183.
14. Laurens N, Koolwijk P, de Maat MPM. Fibrin structure and wound healing. *J Thromb Haemost* 2006;**4**(5):932–9. https://doi.org/10.1111/j.1538-7836.2006.01861.x.
15. Lloyd JM, McIver CM, Stephenson S-A, Hewett PJ, Rieger N, Hardingham JE. Identification of early-stage colorectal cancer patients at risk of relapse post-resection by immunobead reverse transcription-PCR analysis of peritoneal lavage fluid for malignant cells. *Clin Cancer Res* 2006;**12**(2):417–23. https://doi.org/10.1158/1078-0432.CCR-05-1473.
16. Lopez-Alemany R, Mirshahi F, Burtin P, Soria C, Soria N, Faure JP, Mirshahi M. Generation and characterization of monoclonal antibodies against plasmin receptor from human carcinoma cells. *Fibrinolysis* 1994;**8**:54. https://doi.org/10.1016/0268-9499(94)90434-0.
17. McDonald JA, Quade BJ, Broekelmann TJ, LaChance R, Forsman K, Hasegawa E, Akiyama S. Fibronectin's cell-adhesive domain and an amino-terminal matrix assembly domain participate in its assembly into fibroblast pericellular matrix. *J Biol Chem* 1987;**262**(7):2957–67.
18. McDonald JA. Extracellular matrix assembly. *Annu Rev Cell Biol* 1988;**4**(1):183–207. https://doi.org/10.1146/annurev.cb.04.110188.001151.
19. Mirshahi M, Soria J, Soria C, Perrot J-Y, Boucheix C. A latex immunoassay of fibrin/fibrinogen degradation products in plasma using a monoclonal antibody. *Thromb Res* 1986;**44**(6):715–28. https://doi.org/10.1016/0049-3848(86)90018-6.
20. Mistry CD. The beginning of icodextrin. *Perit Dial Int* 2020;49–52. https://doi.org/10.3747/pdi.2009.00217.
21. Moretti FA, Chauhan AK, Iaconcig A, Porro F, Baralle FE, Muro AF. A major fraction of fibronectin present in the extracellular matrix of tissues is plasma-derived. *J Biol Chem* 2007;**282**(38):28057–62. https://doi.org/10.1074/jbc.M611315200.
22. Olszowska, Anna, Jacek Waniewski, Joanna Stachowska-Pietka, Elvia Garcia-Lopez, Bengt Lindholm, Zofia Wan¨kowicz. 2019. Long peritoneal dialysis dwells with icodextrin: kinetics of transperitoneal fluid and polyglucose transport. Front Physiol 10 (october). https://doi.org/10.3389/fphys.2019.01326.
23. Oosterling SJ, van der Bij GJ, van Egmond M, van der Sijp JRM. Surgical trauma and peritoneal recurrence of colorectal carcinoma. *Eur J Surg Oncol (EJSO)* 2005;**31**(1):29–37. https://doi.org/10.1016/j.ejso.2004.10.005.
24. Reymond MA, Hu B, Garcia A, Reck T, KÎckerling F, Hess J, Morel P. Feasibility of therapeutic pneumoperitoneum in a large animal model using a microvaporisator. *Surg Endosc* 2000;**14**(1):51–5. https://doi.org/10.1007/s004649900010.
25. Rosowski E, Huttenlocher A. Neutrophils, wounds, and cancer progression. *Dev Cell* 2015;**34**(2):134–6. https://doi.org/10.1016/j.devcel.2015.07.005.
26. Ruoslahti E. Fibronectin and its integrin receptors in cancer. *Adv Cancer Res* 1999;**76**:1–20. https://doi.org/10.1016/s0065-230x(08)60772-1.
27. SÄnchez-Hidalgo JM, RodrÔguez-Ortiz L, Arjona-SÄnchez à, RufiÄn-Pe·a S, Casado-Adam à, Cosano-àlvarez A, Brice·o-Delgado J. Colorectal peritoneal metastases: optimal management review. *World J Gastroenterol* 2019;**25**(27):3484–502. https://doi.org/10.3748/wjg.v25.i27.3484.
28. Schlag G, Redl H, Turnher M, Dinges HP. 1986. The importance of fibrin in wound repair. In Fibrin sealant in operative medicine, ÅditÅ par GÏnther Schlag et Heinz Redl, 3⊠12. Berlin, Heidelberg: Springer. https://doi.org/10.1007/978-3-642-82880-5_1.
29. Shahid S, Iman A, Matti U, Rachid K, Assaf A, Eveno C, Marc P, Massoud M. Fibrin deposit on the peritoneal surface serves as a niche for cancer expansion in carcinomatosis patients. *Neoplasia* 2019;**21**(11):1091–101. https://doi.org/10.1016/j.neo.2019.08.006.
30. Song, Xu, Fengmin Wang, Haibo Shen, Jie Li, Tianjun Hu, Zhenhua Yang, Yinjie Zhou, Qiang Shi. 2019. [Correlation between Plasma D-dimer Count and Features of Non-small Cell Lung Cancer]. Zhongguo Fei Ai Za Zhi = Chinese J Lung Cancer 22 (3): 151⊠56. https://doi.org/10.3779/j.issn.1009-3419.2019.03.06.
31. Soria J, Soria C, Mirshahi M, Boucheix C, Aurengo A, Perrot J-Y, Bernadou A, Samama M, Rosenfeld C. Conformational change in fibrinogen induced by adsorption to a surface. *J Colloid Interface Sci* 1985;**107**(1):204–8. https://doi.org/10.1016/0021-9797(85)90163-8.
32. Sugarbaker PH. Intraperitoneal chemotherapy and cytoreductive surgery for the prevention and treatment of peritoneal carcinomatosis and sarcomatosis. *Semin Surg Oncol* 1998;**14**(3):254–61. https://doi.org/10.1002/(SICI)1098-2388(199804/05)14:3<254::AID-SSU10>3.0.CO;2-U.
33. Takebayashi K, Murata S, Yamamoto H, Ishida M, Yamaguchi T, Kojima M, Shimizu T, et al. Surgery-induced peritoneal cancer cells in patients who have undergone curative gastrectomy for gastric cancer. *Ann Surg Oncol* 2014;**21**(6):1991–7. https://doi.org/10.1245/s10434-014-3525-9.
34. Tempfer CB, Celik I, Solass W, Buerkle B, Pabst UG, Zieren J, Strumberg D, Reymond M-A. Activity of Pressurized Intraperitoneal Aerosol Chemotherapy (PIPAC) with cisplatin and doxorubicin in women with recurrent, platinum-resistant ovarian cancer: preliminary clinical experience. *Gynecol Oncol* 2014;**132**(2):307–11. https://doi.org/10.1016/j.ygyno.2013.11.022.

35. To WS, Midwood KS. Plasma and cellular fibronectin: distinct and independent functions during tissue repair. *Fibrogenesis Tissue Repair* 2011;**4** (september):21. https://doi.org/10.1186/1755-1536-4-21.
36. Tokumitsu Y, Yoshino S, Iida M, Yoshimura K, Ueno T, Hazama S, Oka M. Intraoperative dissemination during gastrectomy for gastric cancer associated with serosal invasion. *Surg Today* 2015;**45**(6):746–51. https://doi.org/10.1007/s00595-014-1005-2.
37. van den Tol PM, van Rossen EEM, van Eijck CHJ, Bonthuis F, Marquet RL, Jeekel H. Reduction of peritoneal trauma by using nonsurgical gauze leads to less implantation metastasis of spilled tumor cells. *Ann Surg* 1998;**227** (2):242–8. https://doi.org/10.1097/00000658-199802000-00014.
38. Ullah M, Azazzen D, Kaci R, Benabbou N, Pujade Lauraine E, Pocard M, Mirshahi M. High Expression of HLA-G in ovarian carcinomatosis: the role of interleukin-1β. *Neoplasia (New York, NY)* 2019;**21**(3):331–42. https://doi.org/10.1016/j.neo.2019.01.001.
39. VarjÇ I, Longstaff C, SzabÆ L, Farkas àZ, Varga-SzabÆ VJ, Tanka-Salamon R, Machovich R, Kolev K. DNA, histones and neutrophil extracellular traps exert anti-fibrinolytic effects in a plasma environment. *Thromb Haemost* 2015;**113**(06):1289–98. https://doi.org/10.1160/TH14-08-0669.
40. Petersen W, Colmers-Bruns F. Anatomische und klinische Untersuchungen Ïber die Magen-und Darm-carcinome. *BeitrÌge Zur Klin Chir* 1904;**1904**.
41. Wang Y, Carrim N, Ni H. Fibronectin orchestrates thrombosis and hemostasis. *Oncotarget* 2015;**6**(23):19350–1.
42. Wang Y, Reheman A, Spring CM, Kalantari J, Marshall AH, Wolberg AS, Gross PL, et al. Plasma fibronectin supports hemostasis and regulates thrombosis. *J Clin Invest* 2014;**124**(10):4281–93. https://doi.org/10.1172/JCI74630.
43. Yang L, Liu Q, Zhang X, Liu X, Zhou B, Chen J, Huang D, et al. DNA of neutrophil extracellular traps promotes cancer metastasis via CCDC25. *Nature* 2020;**583**(7814):133–8. https://doi.org/10.1038/s41586-020-2394-6.
44. Yee-Moon Wang, Angela. 2019. 31 - Peritoneal dialysis solutions, prescription and adequacy. In Chronic Kidney disease, dialysis, and transplantation (Fourth Edition), ÅditÅ par Jonathan Himmelfarb et T. Alp Ikizler, 480-508.e9. Philadelphia: Elsevier. https://doi.org/10.1016/B978-0-323-52978-5.00031-8.
45. Zeamari S, Roos E, Stewart FA. Tumour seeding in peritoneal wound sites in relation to growth-factor expression in early granulation tissue. *Eur J Cancer* 2004;**40**(9):1431–40. https://doi.org/10.1016/j.ejca.2004.01.035.